LINEAR ELECTRON ACCELERATION IN THz WAVEGUIDES *

E. A. Nanni†, W. S. Graves, K.-H. Hong, W. R. Huang, K. Ravi, L. J. Wong, MIT, Cambridge, USA
G. Moriena, University of Toronto, Toronto, Canada, A. Fallahi, CFEL, Hamburg, Germany
R. J. D. Miller, Max Planck Institute for the Structure and Dynamics of Matter, Hamburg, Germany, and the University of Toronto, Toronto, Canada
F. X. Kärtner, CFEL, Hamburg, Germany and MIT, Cambridge, USA

Abstract

We report the first experimental demonstration of linear electron acceleration using an optically generated single-cycle THz pulse centered at 0.45 THz. 7 keV of acceleration is achieved using 10 μJ THz pulses in a 3 mm interaction length. The THz pulse is produced via optical rectification of a 1.2 mJ, 1 μm laser pulse with a 1 kHz repetition rate. The THz pulse is coupled into a dielectric-loaded circular waveguide with 10 MeV/m on-axis accelerating gradient. A 25 fC input electron bunch is produced with a 60 keV DC photo-emitting cathode. The achievable accelerating gradient in the THz structures being investigated will scale rapidly by increasing the IR pulse energy (100 mJ - 1 J) and correspondingly the THz pulse energy. Additionally, with recent advances in the generation of THz pulses via optical rectification, in particular improvements to efficiency and generation of multi-cycle pulses, GeV/m accelerating gradients could be achieved. An ultra-compact high-gradient THz accelerator would be of interest for a wide variety of applications.

INTRODUCTION

Compact high-gradient accelerators are of interest for a wide variety of applications such as free electron lasers, medical linear accelerators (LINAC) and future colliders. Accelerating structures that operate in the THz frequency band are one possible approach to obtaining gradients well above the 30-50 MV/m achieved in conventional LINACs [1]. Increasing the operational frequency into the THz band allows for greatly increased accelerating gradients due to reduced high voltage breakdown and pulsed heating. With recent advances in the generation of THz pulses via optical rectification (OR), in particular improvements in efficiency [2–4] and multi-cycle pulse generation [5], increasing accelerating gradients by two orders of magnitude over conventional RF LINACs operating at GHz frequencies has become a possibility. The results presented in this article demonstrate the development of an ultra-compact high-gradient accelerator that is capable of being scaled to high energy and is compatible as an add-on to existing LINACs.

At RF frequencies where conventional sources (klystrons, etc.) are efficient, surface electric field gradients in accelerating structures are limited by RF induced breakdown. Empirically, the breakdown threshold has been found [6, 7] to scale as

$$E_s \propto \frac{f^{1/2}}{\tau^{1/4}} \tag{1}$$

where E_s is the surface electric field, f is the frequency of operation and τ is the pulse length. Additionally, low frequencies inherently require long RF pulses because a single RF cycle is long (on the order of ns) and traditional sources work most efficiently when operating over a very narrow frequency spectrum (i.e. long pulse length). Presently available laser technology (100 mJ – 1 J pulses) would allow for the production of extremely high gradients with compressed broad-bandwidth pulses [8]. However, infrared and optical wavelengths are difficult to use for the acceleration of electrons with significant charge per bunch due to the short wavelength. Additionally, in order to prevent emittance growth due to increased energy spread, the electron bunch needs to occupy a small fraction of the optical cycle. Difficulties increase when considering the available options for guiding the optical light in order to decrease the phase velocity to match the electron velocity. A guided mode at 10 μm would require sub-micron precision for aligning the electron bunch and the optical waveguide.

THz frequencies provide us with the best of both worlds; the wavelength is long enough that we can fabricate waveguides, provide accurate timing and a significant amount of charge per bunch, while the frequency is high enough that the RF breakdown threshold is increased into the GV/m range. The surface electric field limit should be approaching the maximum surface electric field of 7 GV/m [9], corresponding to the field which induces a tensile stress that is equal to the tensile strength for the copper. Additionally, using optical generation techniques we can have very short THz pulses (~100 ps) which limits pulsed heating and the average power load, leading to high repetition rates (on the order of kHz and above). In Eqn. (1) we can see that both the increase in operational frequency as well as the reduction in pulse length will play a role in increasing the breakdown limit. For the THz structures being considered, the waveguide aperture is ~1 mm and the accelerating gradient is uniform in the transverse dimension. This allows beams on the order of hundreds of microns, easing restrictions on transverse alignment and effects from space charge.

HIGH INTENSITY THz PULSES

The THz pulse which is used in the accelerating structure is generated with OR of 700 fs, 1 μm pulses in cryo-

* Supported by DARPA N66001-11-1-4192, CFEL DESY, DOE DE-FG02-10ER46745, DOE DE-FG02-08ER41532, ERC Synergy Grant 609920 and NSF DMR-1042342.
† enanni@mit.edu

genically cooled Lithium Niobate (LN). The THz pulse is centered at 0.45 THz with a broad spectrum ranging from 0.2 – 0.8 THz. A pulse energy of 10 μJ is produced from 1.2 mJ of IR which is slightly lower than the peak conversion efficiency of THz generation due to a larger spot size in the LN (decreased fluence) for improved transport of the THz beam. The THz beam, shown in Fig. 1(a), has excellent Gaussian mode content which allows for low-loss coupling.

Electro-optic (EO) sampling was used to determine the spectral properties of the THz pulse and the dispersion induced from the quasi-optical elements in the THz beamline. Optical synchronization between the THz pulse and a mode-locked fiber oscillator (80 MHz, 70 fs, 1030 nm) was ensured because it is also the seed for the regenerative amplifier which is used for generating the THz pulses. Birefringence was induced in a 200 μm thick, 110-cut ZnTe crystal. The THz pulse is shown in the time and frequency domain in Fig. 1(b).

The THz pulse is linearly polarized, which is not compatible with the TM_{01} mode used in the accelerating structure. A segmented half waveplate with quasi-continuous variation in the direction of the crystal axis was used to convert the linearly-polarized light to radially-polarized light. Each segment of the waveplate imparts the appropriate rotation to the polarization transitioning from a linear to a radially-polarized beam which couples well to the TM_{01} mode of the accelerating structure. A segmented waveplate with 8 segments of ~8 mm thick quartz designed for operation at 0.45 THz was used.

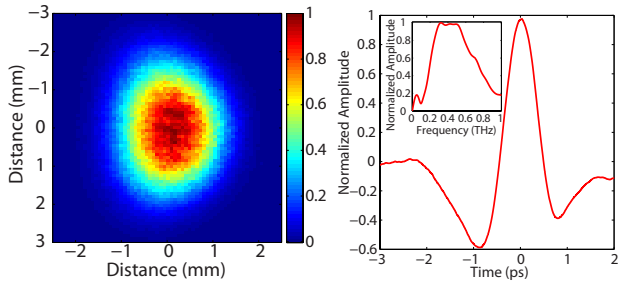

(a) (b)

Figure 1: (a) Normalized intensity of the focused THz beam and (b) the time-domain waveform of the THz pulse determined with EO sampling. Insert: Corresponding frequency-domain spectrum.

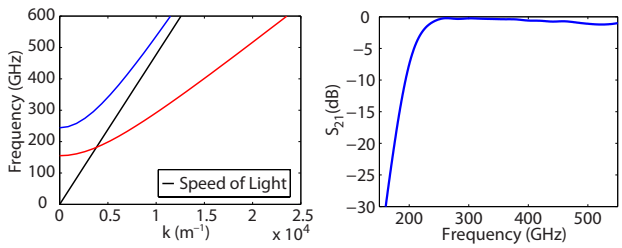

(a) (b)

Figure 2: (a) Dispersion relation for the TM_{01} mode with (red) and without (blue) dielectric loading. (b) The coupling of the free-space radially-polarized mode into the TM_{01} mode through a dielectric-loaded taper.

THz ACCELERATING STRUCTURES

A dielectric-loaded circular waveguide was used as the accelerating structure for the THz LINAC. This waveguide supports a traveling TM_{01} mode that was phase-matched to the velocity of the electron bunch produced by the DC photoinjector. A traveling-wave mode is advantageous when considering coupling of the available single-cycle THz pulse into the structure. A dielectric-loaded circular waveguide was selected due to the ease of fabrication in the THz band. The inner diameter of the copper waveguide is 940 μm with a dielectric wall thickness of 270 μm. This results in a vacuum space with a diameter of 400 μm. The significant thickness of the dielectric is due to the low energy of the electrons entering the structure, and will decrease significantly at higher energy. The dispersion relation for the TM_{01} mode with and without dielectric loading is shown in Fig. 2(a). One critical aspect for THz electron acceleration is proper interaction between the electron beam and the THz pulse. Previously reported work demonstrated that a dielectric-loaded waveguide was a good candidate for an acceleration structure [10]. Coupling the radially polarized THz pulse into the single mode dielectric waveguide was achieved with a centrally loaded dielectric horn. The design was optimized to maximize coupling with minimal fabrication complexity. HFSS simulations indicate excellent coupling of the THz pulse over a ~200 GHz bandwidth, Fig. 2(b), which is compatible with the bandwidth of the radially-polarized mode converter.

Transmission measurements were performed to test and optimize the coupler and waveguide performance. Measurements were performed with a Gentec-EO Pyroelectric Joulemeter Probe that is capable of measuring pulse energies exceeding 100 nJ. Efficient excitation of the TM_{01} mode, demonstrated in these measurements, is a critical requirement in developing a compact high-gradient THz LINAC. Measured transmission efficiencies are compared with theoretical values in Table 1. The vertical and horizontal polarization measured after the segmented waveplate were 53% and 47%, respectively. The waveguide length was 5 cm, including two tapers, demonstrating that ohmic losses are manageable even over significant interaction lengths. With a measured energy of 2 μJ at the exit of the waveguide the calculated on-axis accelerating gradient is 9.7 MeV/m.

Table 1: Transmission for THz Components

Element	Predicted	Measured
Segmented Waveplate	0.71	0.38
Copper Waveguide (TM_{01})	0.69	0.54
Dielectric Waveguide (TM_{01})	0.64	0.32

ISBN 978-3-95450-132-8

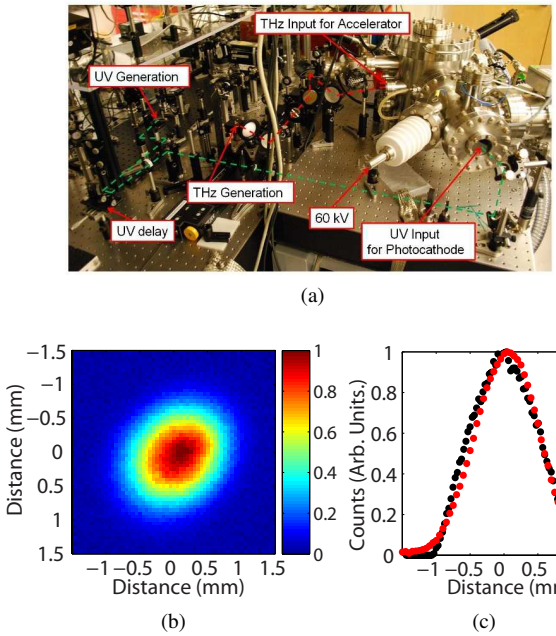

Figure 3: (a) THz LINAC and source with the THz acceleration chamber and accompanying power supplies, chillers and pumps fit on a portable optical cart. (b) Image of the electron beam from an MCP at 50 kV. (c) Comparison between simulated (black) and measured (red) electron bunch at MCP, with 25 fC per bunch, a $\sigma_\perp = 513\mu$m and $\Delta E/E = 1.25$ keV. After the pin-hole the transverse emittance is 25 nm-rad and the longitudinal emittance is 5.5 nm-rad.

THz LINAC

A 60 kV DC photo-emission electron gun was used as the injector for the THz-driven LINAC. Dielectric-loaded circular waveguides, described in the previous section, were optimized for non-relativistic electron beams and used as the acceleration structures. The accelerating waveguide is 10 mm in length, including a single tapered horn for coupling the THz into the waveguide. The electron beam produced by the DC electron gun, shown in Fig. 3(a), operates with 25 fC per bunch at a repetition rate of 1 kHz. The photo-emission laser is a 350 fs UV pulse produced by 4$^{\text{th}}$ harmonic generation from the 1 μm laser. Fig. 3(b) shows an image of the electron beam produced by the MCP camera. A focusing solenoid is used to collimate the beam after the THz LINAC. The electron beam energy is determined via energy-dependent magnetic steering with a dipole located after the accelerator. PARMELA simulations were used to model the DC gun, Fig. 3(c), and the THz LINAC. Alignment between the THz waveguide and the DC gun is provided by a pin-hole aperture in a metal plate with a diameter of 100 μm that abuts the waveguide. The THz pulse is coupled into the waveguide downstream of the accelerator and it propagates the full length of the waveguide before being reflected by the pin-hole aperture, which acts as a short at THz frequencies. After being reflected the THz pulse co-propagates with the electron bunch. The interaction length

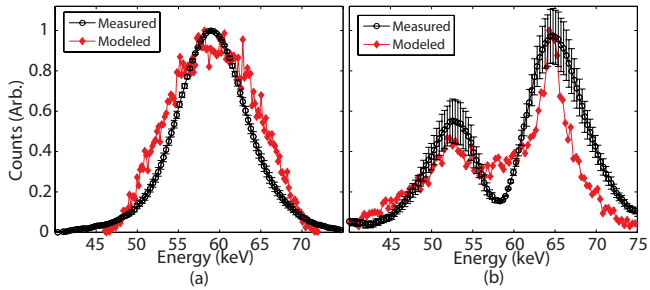

Figure 4: Measured (black) and modeled (red) energy spectrum with THz (a) off and (b) on at a gun voltage of 59 kV.

is limited to 3 mm due to the low initial energy of the electrons which results in the rapid onset of a phase-velocity mismatch between the electron bunch and the THz pulse once the electrons have been accelerated by the THz pulse.

The energy spectrum from the electron bunch with and without THz is shown in Fig. 4 for an initial mean energy of 59 keV. The electron bunch length after the pin-hole, $\sigma_z = 45$ μm, is long with respect to the wavelength of the THz pulse in the waveguide, $\lambda_g = 315$ μm, resulting in both the acceleration and deceleration of particles. The THz waveguide is sensitive to the initial energy of the electron bunch, due to the rapidly varying velocity of the electrons. If the initial energy is too low, acceleration is not observed. With the available THz pulse energy, a peak energy gain of 7 keV was observed by optimizing the electron beam voltage and timing of the THz pulse. The modeled curve in Fig. 4(b) was fit with on on-axis gradient of 4.9 MeV/m, indicating some loss of THz pulse energy due to misalignment. At the exit of the LINAC, the modeled transverse and longitudinal emittance are 240 nm-rad and 370 nm-rad, respectively. This increase in emittance is due to the long electron bunch length compared to the THz wavelength and can be easily remedied with a shorter UV pulse length.

CONCLUSION

THz pulses generated via optical rectification of a 1μm laser were used to accelerate electrons in a simple and practical THz traveling-wave accelerating structure. A gradient of ~10 MeV/m with 2 μJ was achieved during transmission testing. A energy gain of 7 keV was achieved over a 3 mm interaction length. Performance of these structures improves with an increase in electron energy and gradient making them attractive for compact accelerator applications. With upgrades to pump laser energy and technological improvements to THz sources, GeV/m gradients are achievable in dielectric-loaded circular waveguides. The available THz pulse energy scales with IR pump energy, with a recently reported result of 0.4 mJ and ~1% conversion efficiency [11]. Multiple stages of THz acceleration can be used to achieve higher energy gain with additional IR pump lasers for subsequent stages.

REFERENCES

[1] Dolgashev, Valery, et al., "Geometric dependence of radio-frequency breakdown in normal conducting accelerating

structures." Applied Physics Letters 97.17 (2010): 171501.

[2] Huang, Shu-Wei, et al., "High conversion efficiency, high energy terahertz pulses by optical rectification in cryogenically cooled lithium niobate." Optics letters 38.5 (2013): 796-798.

[3] Huang, W. Ronny, et al., "Highly efficient terahertz pulse generation by optical rectification in stoichiometric and cryo-cooled congruent lithium niobate." Journal of Modern Optics ahead-of-print (2014): 1-8.

[4] Ruchert, Clemens, Carlo Vicario, and Christoph P. Hauri, "Spatiotemporal focusing dynamics of intense supercontinuum THz pulses." Physical Review Letters 110.12 (2013): 123902.

[5] Chen, Zhao, et al., "Generation of high power tunable multicycle teraherz pulses." Applied Physics Letters 99.7 (2011): 071102.

[6] Kilpatrick, W. D., "Criterion for vacuum sparking designed to include both rf and dc." Review of Scientific Instruments 28, 824 (1957).

[7] Loew, Gregory A., and J. W. Wang, "RF Breakdown Studies in Room Temperature Electron Linac Structures." 13th Int. Symp. on Discharges and Electrical Insulation in Vacuum, Paris, France. 1988.

[8] Peralta, E. A., et al., "Demonstration of electron acceleration in a laser-driven dielectric microstructure." Nature 503.7474 (2013): 91-94.

[9] Hassanein, A., et al., "Effects of surface damage on rf cavity operation." Physical Review Special Topics-Accelerators and Beams 9.6 (2006): 062001.

[10] Wong, Liang Jie, Arya Fallahi, and Franz X. Kärtner, "Compact electron acceleration and bunch compression in THz waveguides." Optics express 21.8 (2013): 9792-9806.

[11] Fülöp, J. A., et al., "Efficient Generation of THz Pulses with 0.4 mJ Energy", CLEO, SW1F.5, 2014.

ISBN 978-3-95450-132-8